JOURNAL OF APPLIED ELECTROCHEMISTRY 18 (1988) 96–103

Calculation of the current density distribution in an amalgam electrolyser by the finite element method

MICHAL ŠIMEK

Fezko, 386 16 Strakonice, Czechoslovakia

IVO ROUŠAR

Prague Institute of Chemical Technology, Department of Inorganic Technology, 166 28 Prague 6, Czechoslovakia

Received 29 January 1987; revised 29 July 1987

The primary and secondary distribution of current densities at the anode and cathode in an amalgam electrolyser with activated titanium anodes was obtained by solving Laplace's equation by the finite element method. The calculated data were used for evaluation of the decrease of the active layer of RuO_2 around the anode. The results are compared with literature data.

Nomenclature

a	interelectrode distance (cm)
A, B	constants in Tafel equation (V)
c	height of the electrolyte level above anode (cm)
C	constant
E_r	equilibrium potential (V)
I	total current per wire (A)
I_e	current referred to unit length ($A\,cm^{-1}$)
j	current density ($A\,cm^{-2}$)
j^*	current density referred to unit area of projection of the anode into the cathode ($A\,cm^{-2}$)
l	anode length (cm)
m	quantity of Ru in active layer around the anode per unit surface area ($g\,cm^{-2}$)
M	system matrix
$\mathbf{n}$	vector of outer normal (cm)
n_x, n_y	components of unit normal vector (cm)
N	basis functions
p_1, p_2, p_3	constants in equation of parabola
q	rate of decrease of Ru in active layer ($g\,cm^{-2}\,h^{-1}$)
r	anode radius (cm)
$2s$	distance between anodes (cm)
t	time (hour)
u, v	local coordinate system (cm)
U	terminal voltage (V)
U_p	voltage drop in electrode body (V)
w	weight function
x, y	Cartesian (global) coordinates (cm)
α	angle
η	overpotential (V)
π	Ludolf number
ϱ_E	resistivity of electrolyte (Ω cm)
φ	potential (V)
ϕ	dimensionless parameter

Subscripts A – anode, C – cathode
Superscripts N – newly calculated value, s – iteration step

1. Introduction

Amalgam electrolysers with activated titanium anodes are commonly used in the electrolysis of alkali metal chlorides. The activated Ti anodes are represented by a number of parallel wires arranged at given distances. Knowledge of the distribution of current densities around the wires permits determination of the decrease of the active layer at any point. The calculation of the distribution of current densities and total current passing through the electrolyser at various distances between the anode and cathode and between the wires can give information about the efficiency of the electrolysis and about the utilization of the active layer for various electrolyser geometries.

This problem has been dealt with by several authors with different results. For example, the solution presented by Kubasov *et al.* [1] is semiempirical and discontinuous around the circumference of the wires. Loučka *et al.* [2] derived a continuous solution based on a model of a single anode wire and an infinite plane cathode. This solution represents only a rough estimate.

The aim of the present work is to compare the results [2] with a numerical solution of Laplace's equation for a real case taking the influence of neighbouring wires into account. This can be done by several methods [3]. We preferred the method of finite elements, which is recommended for complicated geometries and which partly eliminates some disadvantages of the finite difference and classical variational methods.

2. Experimental details

A cross section of an amalgam electrolyser with activated Ti anodes is shown schematically in Fig. 1. The

0021-891X/88 $03.00 + .12

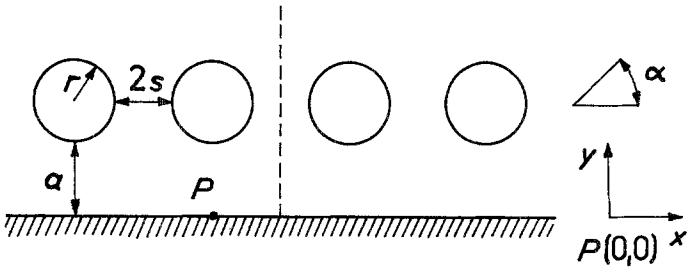

Fig. 1. Schematic cross-section of an amalgam electrolyser with activated Ti anodes. Distance between cathode and anode is denoted as a, origin of x, y coordinates P.

activated Ti anode consists of a number of parallel wires of radius r and length l whose mutual distance is $2s$. The distance between the cathode and the wires (measured at their lowest points) is considered as the interelectrode distance, a. We assume that the composition (and hence also the density and resistivity) of the electrolyte is constant throughout its whole volume.

The problem can be considered as two-dimensional since the properties of the system are constant along the axis parallel to the wires. The origin of coordinates is at the point P, the x axis lies in the cathode surface, and the y axis passes through the anode centre. For further simplification, we take into account the symmetry axis of two neighbouring wires, shown by the dashed line in Fig. 1. Since the properties of the system with a homogeneous medium must be symmetrical with respect to every geometrical symmetry axis, both the dashed line and the y axis have the properties of an insulating wall, on which $\partial\varphi/\partial n = 0$, where n denotes the coordinate normal to the given surface. The solution of the problem is then reduced to calculation of the potential distribution on a region delimited by both symmetry axes, followed by calculation of the current densities at the electrodes.

The distribution of potential, φ, is obtained by solving Laplace's equation

$$\frac{\partial^2\varphi}{\partial x^2} + \frac{\partial\varphi^2}{\partial y^2} = 0 \qquad (1)$$

The individual distances are shown in Fig. 2 (the electrolyte level is at distance c above the anode) together with boundary conditions, the Galvani potential of the electrolyte near the anode (cathode) is denoted as φ_A (φ_C).

To solve Equation (1) by the finite element method, the integration domain is divided into subdomains called finite elements. The solution in each of them is approximated by the same function; this is favourable for assembling a general programme for the solution of this type of problem. Isoparametric parabolic elements were chosen, since they are suitable for domains with curved boundaries. A transformation can be introduced, which permits passing from the global coordinate system (x, y) to a new one (u, v), in which each element is transformed to a square with the centre at the origin of coordinates and side length equal to 2 (Fig. 3). The splitting of the integration domain into finite elements is illustrated in Fig. 4. The division is more detailed at the electrodes, where the potential drop is highest.

In the finite element method, we do not solve Equation (1) directly, but instead we seek a function that minimizes the function corresponding to it, or a function that satisfies the formulation of the problem obtained by the weighted residual method. The latter is used here. We require that the weighted integral of the residue be equal to zero, hence that the residue be orthogonal on the domain Ω with respect to any weight function w, i.e.

$$\int_\Omega \left(\frac{\partial^2\varphi}{\partial x^2} + \frac{\partial^2\varphi}{\partial y^2}\right) w\,d\Omega = 0 \qquad (2)$$

The potential $\varphi(x, y)$ in every finite element is approximated by using the potential values at the nodes, φ_i, and basis functions, $N_i(u, v)$, as

$$\varphi(x, y) = \sum_{i=1}^{8} N_i(u, v)\,\varphi_i \qquad (3)$$

The basis function for a square with side length 2 in the local coordinate system (u, v) can be written as

$$\begin{aligned} N_i &= (1 + uu_i)(1 + vv_i)(uu_i + vv_i - 1)/4 && i = 1\text{–}4 \\ N_i &= (1 - u^2)(1 + vv_i)/2 && i = 5, 7 \\ N_i &= (1 - v^2)(1 + uu_i)/2 && i = 6, 8 \end{aligned} \qquad (4)$$

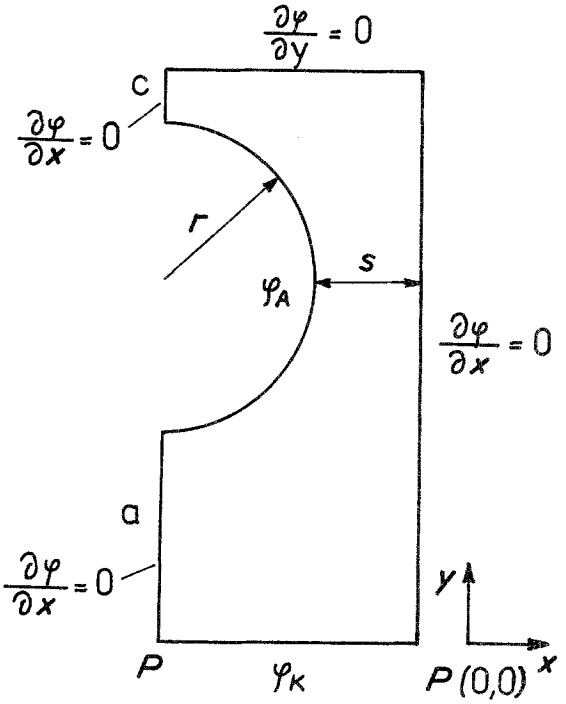

Fig. 2. Integration domain with boundary conditions. ($\varphi_K \equiv \varphi_C$)

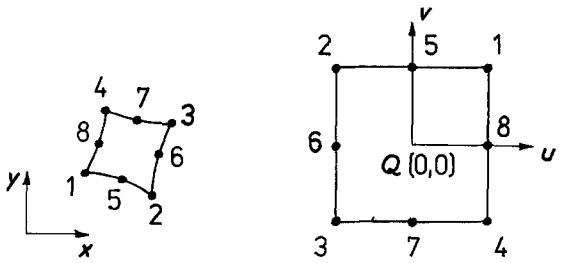

Fig. 3. Parabolic isoparametric element with local indices (1–8) in the global (x, y) coordinate system and after transformation to the local (u, v) one.

where u_i, v_i denote local coordinates of the nodal point.

In Galerkin's method, the basis functions N_i serve at the same time as weight functions. To lower the order of the derivatives in Equation (2), we use Green's theorem for integration by parts of functions of more than one variable [7]

$$-\int\int \Omega\left(\frac{\partial\varphi}{\partial x}\frac{\partial N_j}{\partial x}+\frac{\partial\varphi}{\partial y}\frac{\partial N_j}{\partial y}\right)dx\,dy+\int_\Gamma \frac{\partial\varphi}{\partial n}N_j d=0 \tag{5}$$

Here, the second term need be considered only at the boundary, where nonessential (natural) boundary conditions are prescribed. Since in our case $\partial\varphi/\partial n = 0$ at these boundaries (Fig. 2), the second integral is equal to zero and Equation (5) takes the form

$$\int\int \Omega\left(\frac{\partial\varphi}{\partial x}\frac{\partial N_j}{\partial x}+\frac{\partial\varphi}{\partial y}\frac{\partial N_j}{\partial y}\right)dx\,dy=0 \tag{6}$$

Here, the potential φ is approximated by Equation (3); since the values of φ_i are constant in a chosen element, we obtain

$$\sum_{i=1}^{8}\varphi_i\int\int \Omega\left(\frac{\partial N_i}{\partial x}\frac{\partial N_j}{\partial x}+\frac{\partial N_i}{\partial y}\frac{\partial N_j}{\partial y}\right)dx\,dy=0 \qquad j=1-8 \tag{7}$$

By combining for the whole region Ω, we obtain a system of linear equations, which can be written in the matrix form

$$M\varphi = 0 \tag{8}$$

where M denotes the matrix of the system and φ is the vector of unknown potential values at the nodes (x_i, y_i). The transformation from the local (u, v) to global (x, y) coordinates is given as

$$x=\sum_{i=1}^{8}N_i(u,v)x_i,\quad y=\sum_{i=1}^{8}N_i(u,v)y_i \tag{9}$$

and its uniqueness is secured by the determinant of Jacobi's matrix being different from zero. This determinant is used in calculating the derivatives of the basis functions with respect to global coordinates. Equation (7) is integrated numerically with the aid of Gauss quadrature formula for 3 × 3 points. The values of the integrals are stored in the matrix of the corresponding element and this in turn is used to assemble the matrix of the system. The problem is thus reduced to the solution of a system of linear equations, which are stored in a reduced form in which the zero terms are omitted. The system was solved by the successive over-relaxation method [8].

The potential values in elements adjacent to the electrodes are used in calculating the distribution of the current density j at the boundary. We have

$$j=-\frac{1}{\varrho_E}\frac{\partial\varphi}{\partial n} \tag{10}$$

where ϱ_E is the resistivity of the electrolyte and n the coordinate normal to the boundary. For the cathode, the calculation is simple, since the normal is parallel to the y axis, hence the derivative in Equation (10) can be written as $\partial\varphi/\partial y$. The anode surface, which is circular in cross section, is approximated in the elements by parabolae so that the nodes laying at the apexes of the quadrangles are placed on a circle of radius r and the nodes in the middle of each side have the smallest distance from the circle. The approximation by parabola $y = p_1x^2 + p_2x + p_3$ is also suitable for the determination of the components of the unit normal vector passing through a point x_0:

$$\begin{aligned} n_x &= (p_2+2p_1x_0)/[1+(p_2+2p_1x_0)^2]^{1/2} \\ n_y &= -[1+(p_2+2p_1x_0)^2]^{-1/2} \end{aligned} \tag{11}$$

for $p_1 > 0$. Equation (10) for the current density at point x_0 at the anode then takes the form

$$j_A=-\left(\frac{\partial\varphi}{\partial x}n_x+\frac{\partial\varphi}{\partial y}n_y\right)/\varrho_E \tag{12}$$

It was found that the current densities calculated at the nodes were practically identical with those found

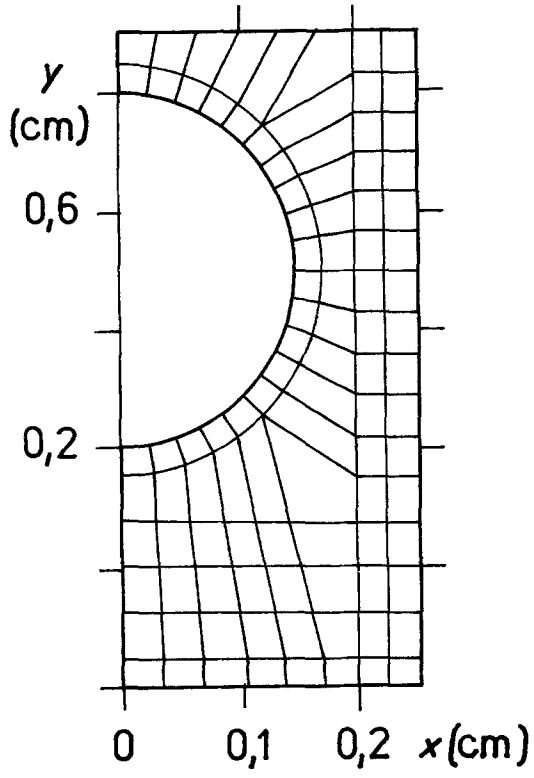

Fig. 4. Division of the integration domain into finite elements.

by extrapolation from the Gauss point inside the element [9], so that the former, simpler method would be used in further calculations.

The total current is obtained by integration of Equation (10) over the electrode surface by means of Gauss three-point quadrature formula. For the planar cathode, the integration is simple. The integral over the arc of a parabola, e.g. between nodes whose x-coordinates are x_1 and x_3, gives the current, $I_{l,A}$, per unit length of the anode

$$I_{l,A} = \int_{x_1}^{x_3} j[1 + (p_2 + 2p_1x)^2]^{1/2}\,dx \qquad (13)$$

The total current passing through one wire of length l is

$$I_A = I_{l,A}l \qquad (14)$$

The correctness of the calculation can be checked by comparing the current flowing through the anode with that flowing through the cathode; they should be equal

$$I_{l,A} = I_{l,C} = I_l \qquad (15)$$

In practice, the mean current density referred to unit area of the projection of the anode into the cathode is of importance:

$$j^* = \frac{I_A}{2(r + s)l} = \frac{I_{l,A}}{2(r + s)} \qquad (16)$$

By combining Equations (12) and (16) we obtain the ratio of j_A/j^*, which characterizes the relative distribution of the current densities at the anode. The analogous ratio j_C/j^* can be derived for the cathode.

The boundary conditions at the electrodes, i.e. potentials in the adjacent electrolyte layer depend on the total imposed voltage, U, on the equilibrium potentials $E_{A,r}$ and $E_{C,r}$, on the overpotential η_A and η_C associated with the electrode reactions, and on the ohmic potential drop in the electrode body, $U_{A,p}$ and $U_{C,p}$. We have

$$\begin{aligned} \varphi_A &= U - U_{A,p} - E_{A,r} - \eta_A \\ \varphi_C &= U_{C,p} - E_{C,r} - \eta_C \end{aligned} \qquad (17)$$

The values of the quantities are taken from the study of the voltage balance of an amalgam electrolyser with activated Ti anodes [10]. For a mean electrolyte temperature of 80° C, mean brine concentration 290 g l^{-1}, and mean concentration of the sodium amalgam 0.1% we obtain

$$\begin{aligned} E_{A,r} &= 1.288\,\text{V} & U_{A,p} &= 0.07\,j^*\,\text{V} \\ E_{C,r} &= -1.753\,\text{V} & U_{C,p} &= 0.007\,j^*\,\text{V} \\ \eta_C &= -0.02 + 0.02\,j_C\,\text{V} \end{aligned} \qquad (18)$$

where j_C is given in A cm^{-2}.

The chlorine overpotential on the activated Ti anode can be approximated by the Tafel equation

$$\eta_A = A + B \log j_A \qquad (19)$$

where the constants were found experimentally to be $A = 0.1$ V, $B = 0.05$ V for $j_A \leqslant 0.32$ A cm^{-2}, and $A = B = 0.15$ V for $j_A > 0.32$ A cm^{-2}.

The resistivity ϱ_E of the electrolyte depends on many factors including hydrodynamic conditions in the electrolyser, however it will be considered constant for the sake of simplicity.

First we deal with the primary distribution of current densities. This corresponds to the ideal case where the polarization of the electrodes is equal to zero ($\eta_A = \eta_C = 0$). We introduce a dimensionless parameter

$$\phi = (E_{C,r} - U_{C,p} + \varphi)/(U - U_{A,p} + E_{C,r} - E_{A,r} - U_{C,p}) \qquad (20)$$

The boundary conditions are $\phi_A = 1$, $\phi_C = 0$. The results obtained by the above-mentioned method will be compared with the solution [2] obtained for one wire (neglecting the influence of the other wires). This rough estimate [2] gives

$$\frac{j_A}{j^*} = \frac{2(r + s)}{2\pi r}\,\frac{[(r + a)^2/r^2 - 1]^{1/2}}{(r + a)/r + \sin\alpha} \qquad (21)$$

$$\frac{j_C}{j^*} = \frac{\sinh\dfrac{\pi[a(2r + a)]^{1/2}}{r + s}}{\cosh\dfrac{\pi[a(2r + a)]^{1/2}}{r + s} - \cos\dfrac{\pi x}{r + s}} \qquad (22)$$

where the meaning of coordinate x and angle α is illustrated in Fig. 1. The total current flowing through a wire is approximated as [2, 11]

$$I = \frac{2\pi(\varphi_A - \varphi_C)}{\varrho_E \ln[(1 + a/r) + ((1 + a/r)^2 - 1)^{1/2}]} \qquad (23)$$

In the case of secondary current distribution, the electrode potential at a given point depends on the current density j. In the first step of numerical calculation, we select values of the electrode potentials corresponding to equations (17) without overpotentials, calculate the current densities, and find the potential values Equation (17) using the equations for the overpotentials Equations (17) and (19). A proportional part of the (inner or Galvani) potential at the nodal point at the electrode (on the electrolyte side) is taken as a new value for further step ($s + 1$);

$$\varphi_{A,C}^{s+1} = C\varphi_{A,C}^{N} + (1 - C)\,\varphi_{A,C}^{s} \qquad (24)$$

The superscript N refers to the newly calculated potential from Equation (17), s denotes last iteration step, and C is an empirical constant which can change during the calculation (in our case $C = 0.05$–0.2). Iteration proceeded until convergence was achieved with an error smaller than 5×10^{-4} V. Provision was made to check whether the potential of the anode under current load was higher than its equilibrium potential.

Gorodetskii *et al.* [12] studied the dependence of decrease of the active layer of Ru and Ti oxides on the current density and found the experimental relationship

$$\log q = -7.57 + 0.30 \log j_A \qquad (25)$$

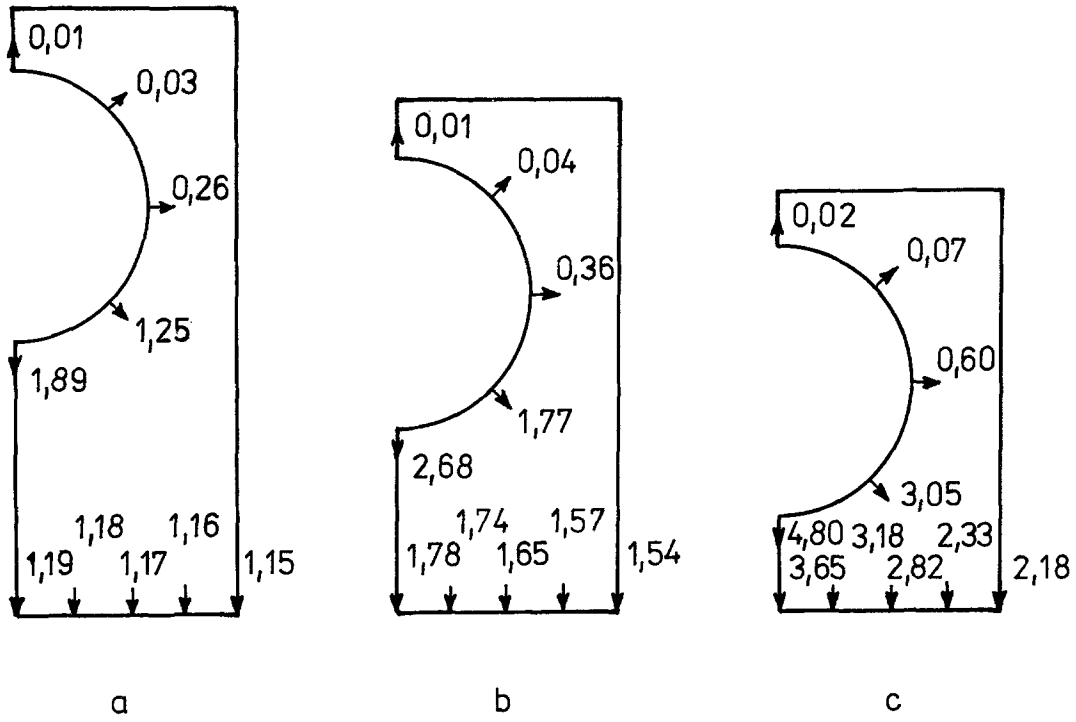

Fig. 5. Primary distribution of current densities at the electrode surface for anode and cathode. Numbers denote c.d. in $A\,cm^{-2}$ for $r = 0.15\,cm$; $s = c = 0.1\,cm$; $\varrho_E = 2.5\,\Omega cm$; values of interelectrode distance a: (a) 0.3 cm; (b) 0.2 cm; (c) 0.1 cm. Arrows indicate the location for given c.d.

where q is the rate of exhaustion of Ru in the active layer. Assuming q constant we obtain the following expression for the quantity, m, of Ru per unit surface area at time t

$$m = m_0 - 2.692.10^{-8} j_A^{0.36} t \qquad (26)$$

The program was assembled in FORTRAN and calculations were made on an ICL-4-72 computer. The region shown in Fig. 4 was divided so that the total number of elements was about 100–110. The calculation of the primary current distribution took about 50 sec of the computer time.

3. Results

The primary distribution of current densities was obtained for an electrolyser with anode wires 3 mm in diameter at various distances between the wires and between the electrodes. The height of the electrolyte level above the anode, c, was found not to influence the total current I, but to influence the local current density at the upper part of the wire surface. In a further calculation, we set $c = 0.1\,cm$. The resistivity ϱ_E of the electrolyte-bubble mixture has no influence on the distribution of the relative current densities, j_A/j^*, and therefore its dependence on the interelectrode distance need not be considered. From the literature [10], its mean value is $\varrho_E = 2.5\,\Omega cm$ at 80° C, brine concentration $290\,g\,l^{-1}$ and for $a = 0.3\,cm$. This was used throughout in the calculation of primary distribution of current densities.

Figure 5 shows the primary distribution of current densities at the electrodes for various interelectrode distances. The distribution of j_A/j^* around the anode and its comparison with Equation (21) neglecting the influence of neighbouring wires [2] is shown in Fig. 6. The distribution of relative current densities calculated by the finite element method is only slightly dependent on the interelectrode distance (other conditions being kept constant), whereas according to the approximation [2] given by Equation (21) it should become more uniform with increasing distance. The mean current density per unit area of the projection of the anode into the cathode, j^*, is, in both methods of calculation, different (Table 1). The dependence of anodic current density distribution on the distance between the wires, $2s$, is shown in Fig. 7. It can be seen that the distribution becomes more nonuniform with increasing distance, since the current increases and j^* decreases as a result of the larger area of the projection of the anode into the cathode. Also here, the values of j^* for both methods of calculation are markedly different (Table 2).

The variation of current at the mercury cathode is shown in Fig. 8 in comparison with approximation [2] given by Equation (22) for x changing from $-(r + s)$ to $r + s$, which corresponds to the projection of the anode into the cathode. The primary distribution of current densities calculated numerically is more nonuniform than according to the estimate [2] given by

Table 1. Mean current density j^* referred to the area of projection of the anode into the cathode for various interelectrode distances (of Fig. 6)

a, cm	0.1	0.2	0.3	0.4
j^*, $A\,cm^{-2}$ (f.e. method)	2.85	1.65	1.17	0.90
j^*, $A\,cm^{-2}$ (approximation by Equations (16) and (23))	4.58	3.37	2.86	2.55

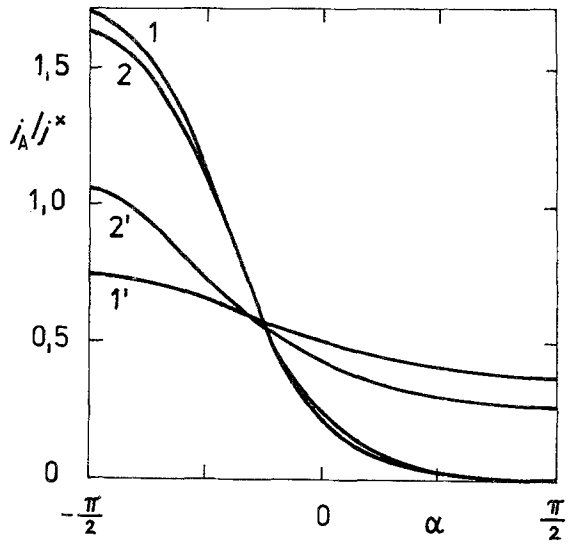

Fig. 6. Primary distribution of relative current densities around the anode wire at various interelectrode distances $r = 0.15$ cm; $c = s = 0.1$ cm; $\varrho_E = 2.5\,\Omega$cm; 1,1′ $a = 0.1$ cm; 2,2′ $a = 0.3$ cm. 1,2 calculated by the finite element method, 1′,2′ approximation given by Equation (21).

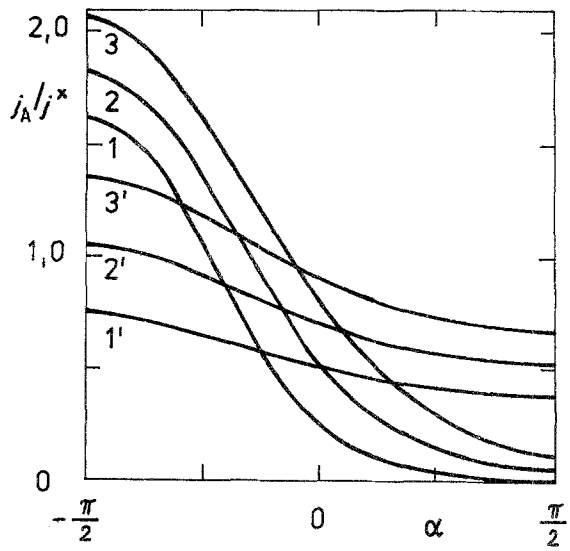

Fig. 7. Primary distribution of relative current densities around the anode wire at various distances between the wires. $r = 0.15$ cm; $a = 0.3$ cm; $c = 0.1$ cm; $\varrho_E = 2.5\,\Omega$cm; 1,1′ $s = 0.1$ cm; 2,2′ $s = 0.2$ cm; 3,3′ $s = 0.3$ cm; 1,2,3 calculated by the finite element method, 1′,2′,3′ approximation given by Equation (21).

Equation (22). In a usual case ($r = 0.15$ cm, $s = 0.1$ cm, $a = 0.3$ cm), the deviation of the local values from the mean current density j^* is approximately 1%. With decreasing interelectrode distance $2s$, the distribution of current densities becomes more nonuniform.

The distribution of Ru as function of time t was calculated from the current densities by using Equation (26) and the results are shown in Fig. 9. The decrease of the active layer is more nonuniform than calculated on the basis of approximation given by Equation (21).

Although the life time of the anode is determined not only by the decrease of the active layer but also by the formation of a nonconducting TiO_2 layer at the Ti-active layer interface, it can be defined for simplicity as the time after which the active layer on the lower part of the wire surface ($\alpha = -\pi/2$) is completely removed. The life thus defined is about the same for both methods of calculation. However, the total charge passed through the electrode during its life time calculated by the finite element method is smaller, since the current, $I = 0.45\,\mathrm{A\,cm^{-1}}$, is lower than that calculated from the approximation given by Equation (23), $I = 1.27\,\mathrm{A\,cm^{-1}}$.

The secondary current distribution was calculated for an electrolyser with wire anodes 3 mm in diameter, distance between the wires $2s = 0.2$ cm, height of electrolyte level above the wires $c = 0.1$ cm, and interelectrode distance $a = 0.2$ or 0.3 cm. The resistivity of the electrolyte-bubble mixture for brine, concentration $290\,\mathrm{g\,l^{-1}}$ at 80° C can be expressed as

$$\varrho_E = 1.836 - 0.2/a \quad (\Omega\mathrm{cm}) \qquad (27)$$

The terminal voltage of the electrolyser was set equal to 4.1 V. The results are shown in Fig. 10 in terms of j_A/j^* around the anode and are compared with the primary current distribution. For primary current density distribution the ratio j_A/j^* is independent of the value $\varphi_A - \varphi_C$ and therefore the results for $\phi_A = 1$ and $\phi_C = 0$ could be used also for $U = 4.1$ V. As expected, the secondary distribution is more uniform than the primary one and the ratio of j_A/j^* is

Table 2. Mean current density j^* referred to the area of projection of the anode into the cathode for various distances between the wire anodes (of Fig. 7)

$2s$, cm	0.2	0.4	0.6
j^*, $\mathrm{A\,cm^{-2}}$ (f.e. method)	1.17	1.07	0.98
j^*, $\mathrm{A\,cm^{-2}}$ (approximation by Equations (16) and (23))	2.86	2.04	1.58

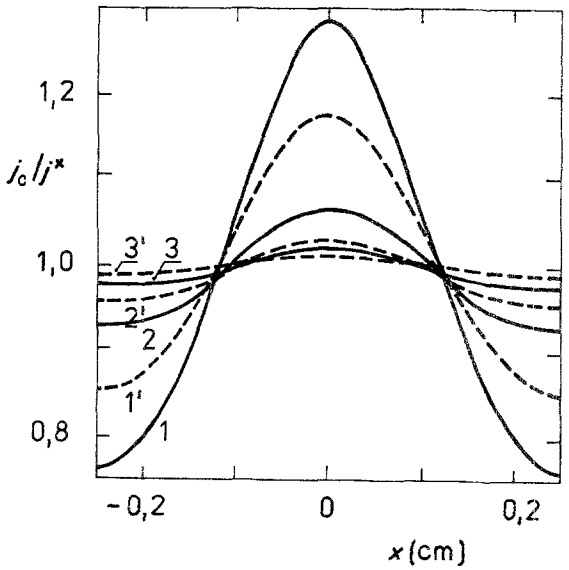

Fig. 8. Primary distribution of relative current densities at the cathode. $r = 0.15$ cm; $c = s = 0.1$ cm; $\varrho_E = 2.5\,\Omega$cm; 1,1′ $a = 0.1$ cm; 2,2′ $a = 0.2$ cm; 3,3′ $a = 0.3$ cm; 1,2,3 calculated by the finite element method, 1′,2′,3′ approximation given by Equation (22).

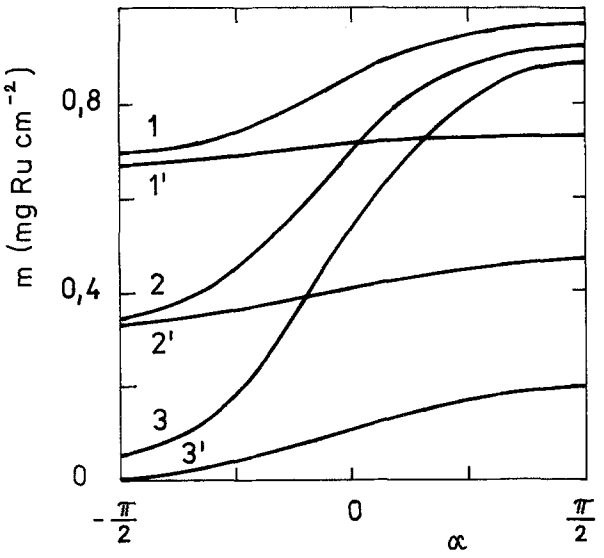

Fig. 9. Distribution of Ru around the wire anode according to Equation (26). $r = 0.15$ cm; $s = c = 0.1$ cm; $a = 0.4$ cm; $\varrho_E = 2.5\,\Omega$cm; $m_0 = 10^{-3}$ g cm^{-2}; 1,1′ $t = 10^4$ h; 2,2′ $t = 2.10^4$ h; 3,3′ $t = 3.10^4$ h; 1,2,3 current density calculated by the finite element method; 1′,2′,3′ approximation given by Equation (21). Primary current density distribution.

only slightly dependent on the interelectrode distance (at constant distance between the wires $2s$).

The correctness of the results can be judged on the basis of the literature data [10]. The terminal voltage of a pilot scale 22 kA electrolyser SCR-22 at 80° C can be expressed as

$$U = 3.105 + (0.415 + 1.8\,a)j^* \qquad (28)$$

(brine concentration 290 g l^{-1}, amalgam concentration 0.1%). For $U = 4.1$ V, $a = 0.2$ cm ($\varrho_E = 2.84\,\Omega$cm) or 0.3 cm ($\varrho_E = 2.5\,\Omega$cm), we find the current density j^* from Equation (28), from the numerical solution by the finite element method (primary and secondary current distribution), and from the estimate given by Equations (16) and (23) with respect to electrode

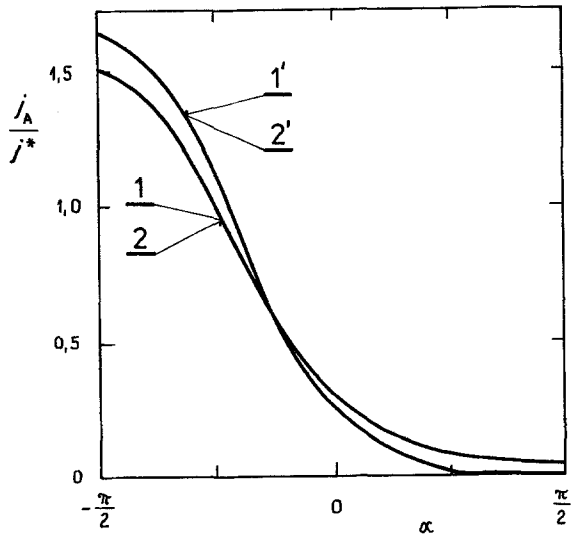

Fig. 10. Distribution of relative current densities around the anode wire calculated by the finite element method. $r = 0.15$ cm; $s = c = 0.1$ cm; $U = 4.1$ V; 1,1′ $a = 0.2$ cm; $\varrho_E = 2.85\,\Omega$cm; 2,2′ $a = 0.3$ cm; $\varrho_E = 2.5\,\Omega$cm; 1,2 secondary distribution; 1′,2′ primary distribution.

polarization and the published data [10]. The calculation of j^* by the finite element method for $U = 4.1$ V and for primary current distribution was carried out using the following procedure. For $a = 0.2$ cm, $\varrho_E = 2.84\,\Omega$cm and primary current distribution we obtained, by solving Laplace's equation for a 1 V potential drop between anode and cathode ($\varphi_A - \varphi_C = 1$ V), $j^* = 1.456$ A cm^{-2}. From Equations (17) and (18) for $\eta_A = \eta_C = 0$ we obtain

$$\varphi_A - \varphi_C = 1.059 - 0.077j^* \qquad (29)$$

Then

$$j^* = 1.456\,(1.059 - 0.077j^*) \qquad (30)$$

which gives $j^* = 1.39$ A cm^{-2}. The potential drop between anode and cathode from Equation (29) is $\varphi_A - \varphi_C = 0.952$ V.

The same procedure was carried out for $a = 0.3$ cm and $\varrho_E = 2.5\,\Omega$cm. For $\varphi_A - \varphi_C = 1$ V the current density $j^* = 1.168$ A cm^{-2} and from Equation (29) we have

$$j^* = 1.168\,(1.059 - 0.077j^*) \qquad (31)$$

In this case $j^* = 1.14$ A cm^{-2} and $\varphi_A - \varphi_C = 0.971$ V.

For the estimate of j^* for $U = 4.1$ V and for the secondary current distribution from Equations (16) and (23) we must take into account the overpotentials η_A and η_C. They are given in [10] by

$$\eta_A = 0.051 + 0.106j^*$$
$$\eta_C = -0.02 - 0.02j^* \qquad (32)$$

From Equations (17) we then obtain

$$\varphi_A - \varphi_C = 0.988 - 0.203j^* \qquad (33)$$

By combining Equations (23), (16) and (33) we obtain for $a = 0.2$ cm, $j^* = 1.83$ A cm^{-2} (the potential drop between anode and cathode $\varphi_A - \varphi_C = 0.617$ V) and for $a = 0.3$ cm, $j^* = 1.79$ A cm^{-2} ($\varphi_A - \varphi_C = 0.626$ V). All these results are summarized in Table 3.

From Table 3 it follows that the values of mean current densities (j^*) obtained experimentally [10] agree approximately (+ 10%, − 15%) with the values computed by the finite element method for primary and secondary current distribution. The values of mean current densities (j^*) calculated according to the approximation using Equations (16) and (23) with polarization of electrodes are much higher (+40%, +80%) than the experimental values or values calculated by the finite element method.

Table 3. Mean current density j^* for various interelectrode distances (see text for details)

a, cm	0.2	0.3
j^*, A cm^{-2} (Eq. (28), experiment [10])	1.28	1.04
j^*, A cm^{-2} (f.e. method, primary current distribution)	1.39	1.14
j^*, A cm^{-2} (f.e. method, secondary current distribution)	1.12	0.94
j^*, A cm^{-2} (approximation by Equations (16) and (23) with polarization of electrodes)	1.83	1.79

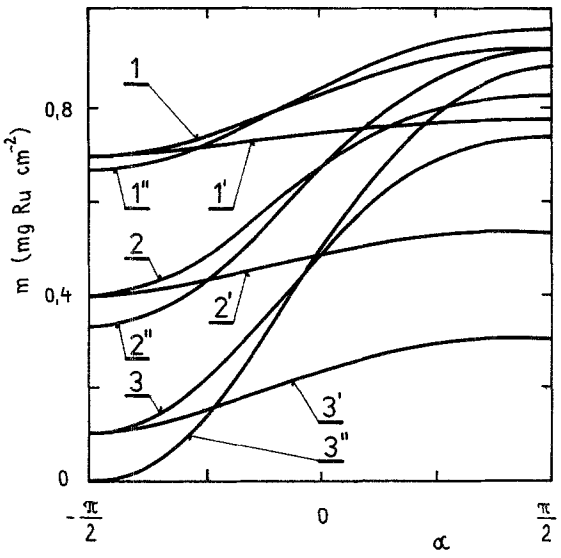

Fig. 11. Distribution of Ru around the wire anode according to Equation (26). $r = 0.15$ cm; $s = c = 0.1$ cm; $a = 0.3$ cm; $\varrho_E = 2.5\,\Omega$cm; $m_0 = 10^{-3}$ g cm^{-2}; $U = 4.1$ V; 1,1',1'' $t = 10^4$ h; 2,2',2'' $t = 2.10^4$ h; 3,3',3'' $t = 3.10^4$ h; 1,2,3 using the secondary distribution of current densities calculated by the finite element method; 1',2',3' using the primary distribution calculated by the finite element method ($\varphi_A - \varphi_C = 0.971$ V); 1'',2'',3'' using current densities according to the approximation given by Equation (21) involving polarization of electrodes ($\varphi_A - \varphi_C = 0.626$ V).

Since an equation of the local anodic polarization curve for the pilot-scale electrolyser used was not available, the overpotential was approximated by the Tafel equation (19) obtained from measurements on laboratory electrodes. Its values are higher than for the pilot-scale electrolyser, hence the values of j^* are somewhat too low.

The secondary distribution of current densities around the anodes can be used to calculate the distribution of ruthenium as function of time as in the preceding case. The results are shown in Fig. 11, where the distributions of Ru calculated from the primary current distribution ($\varphi_A - \varphi_C = 0.971$ V) and the approximation given by Equation (21) involving electrode polarization ($\varphi_A - \varphi_C = 0.626$ V) are also shown for comparison. The curves are in accord with the above conclusion. The distribution of Ru in the active layer calculated from the primary current distribution is very nonuniform. At the lowest part of the wire surface ($\alpha = -\pi/2$) the current densities from the secondary distribution and from Equation (21) involving polarization of the electrodes are the same, hence the calculated Ru content at this place must also be the same.

4. Conclusions

The distribution of current densities around the activated Ti wire anodes in a brine electrolyser was calculated by the finite element method and it was found to be influenced appreciably by the distance between the wires. The previous solution [2] of the Laplace equation around the wire, neglecting the effect of neighbouring wires, does not give reliable results because the calculated current densities referred to unit area of the projection of the anode onto the cathode are in this case much higher compared to a real system [10] and to the calculated values based on the finite element method. The results obtained by the finite element method are in agreement with measurements on a pilot-scale electrolyser [10].

References

[1] V. L. Kubasov, V. Z. Grebenik and R. I. Izosenko, *Chim. prom.* **5** (1980) 289.
[2] Z. Loučka, Z. Ternbachová and F. Moudrý, *Chem. průmysl* **32** (1982) 627.
[3] I. Roušar, K. Micka and A. Kimla, *Electrochemical Engineering*, Vols 1 and 2, Academia, Praha and Elsevier, Amsterdam (1986).
[4] O. C. Zienkiewicz, 'The Finite Element Method in Engineering Science', McGraw-Hill, London (1971).
[5] T. J. Chung, 'Finite Element Analysis in Fluid Dynamics', McGraw-Hill, London (1978).
[6] J. J. Connor and C. A. Brebbia, 'Finite Element Techniques for Fluid Flow', Butterworth, London (1976).
[7] K. Rektorys, 'Přehled užité matematiky'. SNTL, Praha (1968).
[8] H. R. Schwarz, H. Rutishauser and E. Stiefel, 'Numerik symmetrischer Matrizen', B. G. Teubner, Stuttgart (1968).
[9] E. Hinton and J. S. Campbell, *Int. J. for Numerical Methods in Engineering* **8** (1974) 461.
[10] Z. Ternbach and T. Loučka, *Chem. průmysl* **29** (1979) 235.
[11] D. J. Pickett, 'Electrochemical Reactor Design', Elsevier, Amsterdam (1977).
[12] V. V. Gorodestskii, M. M. Pecherskii, V. B. Yanke, P. M. Shub and V. V. Losev, *Elektrochimija* **15** (1979) 559.